
Dynamics of Planetary Rings

Bruno Sicardy^{1,2}

¹ Observatoire de Paris, LESIA, 92195 Meudon Cédex, France
bruno.sicardy@obspm.fr

² Université Pierre et Marie Curie, 75252 Paris Cédex 05, France

Abstract. Planetary rings are found around all four giant planets of our solar system. These collisional and highly flattened disks exhibit a whole wealth of physical processes involving microscopic dust grains, as well as meter-sized boulders. These processes, together with ring composition, can help to understand better the formation and evolution of proto-satellite and proto-planetary disks in the early solar system. The present chapter reviews some fundamental aspects of ring dynamics, namely their flattening, their stability against proper modes, their particle sizes, and their responses to resonance forcing by satellites. These concepts will be used and tested during the forthcoming exploration of the Saturn system by the *Cassini* mission.

1 Introduction

Planetary rings consist in thin disks of innumerable colliding particles revolving around a central planet. They are found around all the four giant planets of our solar system, Jupiter, Saturn, Uranus and Neptune. Meanwhile, they exhibit a wide variety of sizes, masses and physical properties. Also, they involve many different physical processes, ranging from large spiral waves akin to galactic structures, down to microscopic electromagnetic forces on charged dust grains.

All these effects have a profound influence on the long term evolution of rings. As such, they can teach us something about the origin of rings, i.e. whether they are cogenetic to the central planet, or the result of a more recent breakup of a comet or satellite. These processes are also linked to disk dynamics in general, either in proto-planetary circumstellar disks or in galaxies.

A complete review of all these processes remains out of the scope of this short chapter. Instead, we would like to address here a few basic issues related to planetary rings, by asking the following questions:

- Why are planetary rings so flat?

- How thin and dynamically stable are they?
- How do they respond to resonant forcing from satellites?

Answering these questions may help to understand the connection between rings global properties (mass, optical depth, etc. . .) and their local characteristics (particle size and distribution, velocity dispersion, etc. . .).

Extensive descriptions and studies of the issues presented in this chapter are available in the literature. Detailed reviews (and related references) on ring structures, ring dynamics and open issues are presented in [1–6], while ring origin and evolution are discussed in [7] and [8]. Stability issues are discussed in classical papers like [9], and in very much details in reference text books like [10]. Collisional processes are reviewed for instance in [11]. Finally, the various possible responses of disks to resonances and their applications are exposed in [1, 12–14].

2 Planetary Rings and the Roche Zone

Generally speaking, planetary rings reside inside a limit loosely referred to as the ‘Roche zone’ of the central planet. Inside this limit, the tidal stress from the central body tends to disrupt satellites into smaller bodies. Outside this limit, accretion tends to sweep dispersed particles into larger lumps.

Reality is not so sharply defined, though. For instance, the tidal disruption limit for a given body depends not only on the bulk density of that body, which may differ significantly from one body to the other, but also on the tensile strength of that body, another parameter which may vary by several orders of magnitude. Thus, due to these uncertainties, the Roche zone depicted in Fig. 1 remains rather blurred.

In spite of these difficulties, it is instructive to plot the sizes of, say, Saturn’s satellites as a function of their distances to the center of the planet (Fig. 1). Interestingly, one notes that the sizes of the satellites decrease as one approaches the Roche zone, as expected from a simple modelling of tidal stress.

Figure 1 also plots the sizes of satellites that could be formed by lumping together the material of Saturn’s A, B and C rings, as well as of Cassini Division. This figure supports the general idea that the Roche Limit delineates the region inside which tides disrupt solid satellites into a fluid-like ring disk.

Note finally that in the Roche zone, rings and satellites can co-exist, as it is the case for instance for Pan, which orbits inside the Encke Division of Saturn’s A ring. An interesting question is then to know whether satellites and rings can influence each other gravitationally, or even if they can be transformed into each other on long (billions of years) or short (a few years) time scales.

Although Jupiter’s, Uranus’ and Neptune’s rings are much less massive than Saturn’s, they exhibit the same general behavior: smaller and smaller

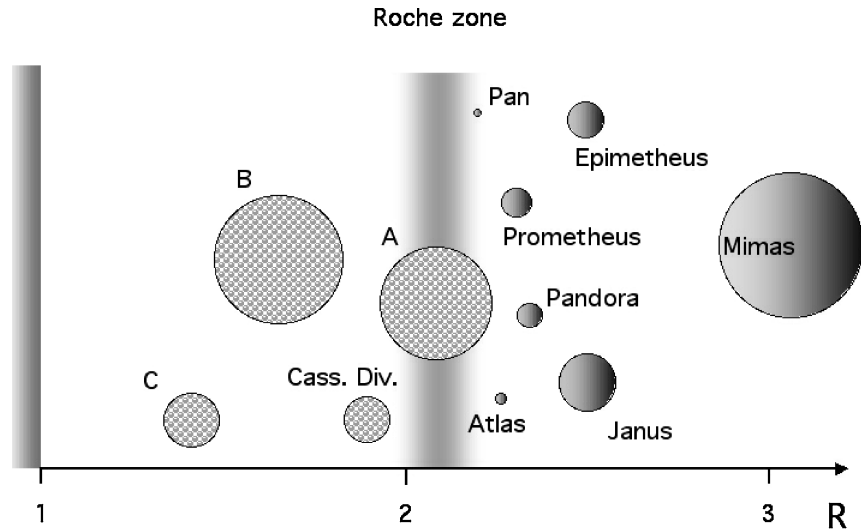


Fig. 1. The relative sizes of Saturn’s inner satellites as a function of their distance to the planet center, in units of the planet radius. The “sizes” of the rings have been calculated by lumping all the material of A, B, C rings and Cassini Division into single bodies. All the sizes have been plotted so that to respect the relative masses of the various bodies involved. For comparison, Mimas has a diameter of about 500 km

satellites are encountered as one approaches the planet Roche zone, then a mixture of rings and satellites is observed, and then only rings are found.

3 Flattening of Rings

Planetary rings flatten because of collisions between particles. This process dissipates mechanical energy, while conserving angular momentum of the ensemble.

Consider a swarm of particles labelled $1, \dots, i, \dots$, with total initial angular momentum \mathbf{H} orbiting a spherical planet centered on O . Let us call the Oz axis directed along \mathbf{H} the “vertical” axis, and the plane Oxy perpendicular to Oz the “horizontal plane”. The orthogonal unit vectors along Ox , Oy and Oz will be denoted $\hat{\mathbf{x}}$, $\hat{\mathbf{y}}$ and $\hat{\mathbf{z}}$, respectively.

Each particle of mass m_i , position \mathbf{r}_i and velocity \mathbf{v}_i has an angular momentum $\mathbf{H}_i = m_i \mathbf{r}_i \times \mathbf{v}_i$, so that:

$$\mathbf{H} = \sum_i m_i \mathbf{r}_i \times \mathbf{v}_i = \sum_i m_i \mathbf{r}_i \times \mathbf{v}_{iz} + \sum_i m_i \mathbf{r}_i \times \mathbf{v}_{ih} ,$$

where \mathbf{v}_{iz} and \mathbf{v}_{ih} are the vertical and horizontal contributions of the velocities, respectively. The vector \mathbf{v}_{ih} can furthermore be decomposed into a

tangential component, $\mathbf{v}_{i\theta}$ and a radial one, \mathbf{v}_{ir} . Projecting \mathbf{H} along the unit vector $\hat{\mathbf{z}}$ along Oz , one gets:

$$H = \mathbf{H} \cdot \hat{\mathbf{z}} = \sum_i m_i (\mathbf{r}_i \times \mathbf{v}_{iz}) \cdot \hat{\mathbf{z}} + \sum_i m_i (\mathbf{r}_i \times \mathbf{v}_{ih}) \cdot \hat{\mathbf{z}} = \sum_i m_i r_i v_{i\theta} .$$

The equality above holds because the first sum vanishes altogether since \mathbf{v}_{iz} and $\hat{\mathbf{z}}$ are parallel, and also because only the tangential velocity survives in the second sum, due to the presence of \mathbf{r}_i in the mixed product $(\mathbf{r}_i \times \mathbf{v}_{ih}) \cdot \hat{\mathbf{z}}$.

On the other hand, the mechanical energy of the ring is given by:

$$E = \sum_i m_i \Phi_P(r_i) + \sum_i m_i v_{i\theta}^2/2 + \sum_i m_i v_{ir}^2/2 + \sum_i m_i v_{iz}^2/2 ,$$

where $\Phi_P(r_i)$ is the planetary potential well per unit mass felt by the particle i .

Comparing the expressions of H and E , one sees that it is possible to minimize the energy E of the ring while conserving the angular momentum H , by simply zeroing v_{ir} and v_{iz} . In other words, the collisions, by dissipating energy while conserving angular momentum, tend to flatten the disk perpendicular to its total angular momentum, and to circularize the particles orbits.

If the planet is not spherically symmetric, as it is the case for all the oblate giant planets, then only the projection of \mathbf{H} along the planet spin axis (say, \mathbf{H}_{spin}) is conserved. The same reasoning as above then shows that the configuration of least energy which conserves \mathbf{H}_{spin} is a flat, but now equatorial ring.

4 Stability of Flat Disks

The considerations presented above lead to the conclusion that a dissipative ring will eventually collapse to an infinitely thin disk with perfectly circular orbits.

In reality, this is not quite true, as some physics is still missing in the description of the rings. For instance, the differential Keplerian motion, combined with the finite size of the particles and the mutual gravitational stirring of the larger particles will maintain a small residual velocity dispersion in the system (i.e. a pressure).

This dispersion induces a small but non-zero thickness of the disk, and is actually necessary to ensure the dynamical stability of the disk versus another destabilizing effect, namely self-gravity.

To quantify this effect, let us describe a planetary ring as a very thin disk where the surface density, velocity and pressure at a given point \mathbf{r} and a given time t will be denoted respectively Σ , \mathbf{v} and p . Furthermore, let Φ_D be the gravitational potential (per unit mass) created by the disk and c_s the speed of sound in the ring, corresponding to the typical velocity dispersion of the particles.

A detailed account of the calculations derived below and their physical interpretations can be found in [10]. In a first step, one can use a toy model where the disk is in *uniform* rotation with constant angular velocity vector $\boldsymbol{\Omega}$ directed along the vertical axis Oz . This will highlight the role of rotation in the stability of the ring, while simplifying the equations of motion. In reality, a disk around a planet exhibits a roughly Keplerian shear ($\Omega \propto r^{-3/2}$), but the conclusions concerning the role of rotation will not be altered in the present, simplified, approach.

The eulerian equations describing the dynamics of the disk are then, in a frame *rotating at angular velocity* Ω :

$$\left\{ \begin{array}{l} \frac{\partial \mathbf{v}}{\partial t} + (\mathbf{v} \cdot \nabla) \mathbf{v} = -\frac{\nabla p}{\Sigma} - \nabla(\Phi_P + \Phi_D) - 2\boldsymbol{\Omega} \times \mathbf{v} + \Omega^2 \mathbf{r} \\ \frac{\partial \Sigma}{\partial t} + \nabla \cdot (\Sigma \mathbf{v}) = 0 \\ \nabla^2 \Phi_D = 4\pi G \Sigma \delta(z) \\ p = \Sigma c_s^2 \end{array} \right. \quad (1)$$

The first line is Euler's equation, where the acceleration on the fluid is expressed in terms of the pressure p , the potentials of the planet and the disk, Φ_P and Φ_D , respectively, the Coriolis term and the centrifugal acceleration. The second line the continuity equation, expressing the conservation of mass. The next line is Poisson's equation, relating the potential Φ_D of an infinitively thin disk to the surface density Σ , the gravitational constant G and the Dirac function $\delta(z)$, where z is the elevation perpendicular to the ring plane. Finally, the last line is the simplest equation of state, that of an isothermal disk, relating the pressure p to the surface density Σ through the speed of sound c_s .

A classical approach is to consider what happens to the disk when small perturbations are applied. For small enough disturbances, the equations above can be linearized, assuming that the unperturbed disk has uniform density. Then the various quantities involved can be decomposed into an unperturbed background value (with index 0) and a small perturbed value (with index 1): $\Phi = \Phi_P + \Phi_{D0} + \Phi_{D1}$, $\Sigma = \Sigma_0 + \Sigma_1$, $\mathbf{v} = \mathbf{0} + \mathbf{v}_1$, $p = p_0 + p_1$.

This leads, after linearization of (1):

$$\left\{ \begin{array}{l} \frac{\partial \Sigma_1}{\partial t} + \Sigma_0 (\nabla \cdot \mathbf{v}_1) = 0 \\ \frac{\partial \mathbf{v}_1}{\partial t} = -\frac{c_s^2}{\Sigma_0} \nabla \Sigma_1 - \nabla \Phi_{D1} - 2\boldsymbol{\Omega} \times \mathbf{v}_1 \\ \nabla^2 \Phi_{D1} = 4\pi G \Sigma_1 \delta(z) \end{array} \right. \quad (2)$$

One can seek how a given disturbance, for instance $\Sigma_1 = \bar{\Sigma}_1 \exp[i(\mathbf{k} \cdot \mathbf{r} - \omega t)]$, propagates in the disk, where $\bar{\Sigma}$ is the amplitude, \mathbf{k} is the wavevector and ω is the frequency of the disturbance (with similar notations for the pressure and velocity). With no loss of generality we can assume that the disturbance propagates in the disk along the horizontal axis Ox , i.e. $\mathbf{k} = k\hat{\mathbf{x}}$.

Partial derivatives with respect to x and t are then equivalent to multiplications by ik and $-i\omega$, respectively. Also, Poisson's equation in the system 2 can be integrated as $|k|\bar{\Phi}_{D1} = -2\pi G\bar{\Sigma}_1$. This provides the algebraic system:

$$\begin{cases} ik\Sigma_0\bar{v}_{1x} & -i\omega\bar{\Sigma}_1 & = 0 \\ i\omega\bar{v}_{1x} & +2\Omega\bar{v}_{1y} + \left(\frac{2\pi G}{|k|} - \frac{c_s^2}{\Sigma_0}\right) ik\bar{\Sigma}_1 & = 0 \\ 2\Omega\bar{v}_{1x} & -i\omega\bar{v}_{1y} & = 0 \end{cases}$$

This system has non trivial solutions only if its determinant is non zero, thus providing the dispersion relation for propagating modes in a uniformly rotating disk:

$$\omega^2 = k^2 c_s^2 - 2\pi G \Sigma_0 |k| + 4\Omega^2 \quad (3)$$

Modes with $\omega^2 < 0$ will be unstable, so that the dispersion relation tells us which wavenumbers are unstable in the disk.

It is instructive to vary the values of c_s and Ω to see the respective effects of pressure and rotation on the stability of a thin (i.e. 2-D) disk. Various cases can be considered:

- *Cold and motionless disk*: $c_s = 0$ and $\Omega = 0$. Then $\omega^2 = -2\pi G \Sigma_0 |k|$, see Fig. 2(a), and all the modes are unstable, as expected, since nothing can stop the gravitational collapse of any disturbance. Note that the free fall collapse time, $t_{\text{colla}} \sim 1/\sqrt{G \Sigma_0 |k|}$ depends on the wavenumber k of the disturbance, the smaller structures collapsing faster than the larger ones. This contrasts with the 3-D case, where the free fall time scale depends only upon the unperturbed density ρ_0 : $t_{\text{colla}} \sim 1/\sqrt{G \rho_0}$.
- *Hot and motionless disk*: $c_s \neq 0$ and $\Omega = 0$. Now $\omega^2 = k^2 c_s^2 - 2\pi G \Sigma_0 |k|$, so that the disk is unstable for disturbances with $|k| < k_J$, where

$$k_J = 2\pi G \Sigma_0 / c_s^2$$

is the Jeans wavenumber, see Fig. 2(b). The relation $|k| < k_J$ is actually the Jeans criterium for a 2-D disk. It can be compared to its 3-D classical counterpart $|k| < k_J = \sqrt{4\pi G \rho_0 / c_s^2}$. This criterium indicates how small the wavenumber must be (i.e. how *large and massive* the disturbance must be) in order to overcome the pressure associated with c_s .

- *Cold rotating disk*: $c_s = 0$ and $\Omega \neq 0$. This yields $\omega^2 = -2\pi G \Sigma_0 |k| + 4\Omega^2$, which shows that now the *large* disturbances (with small k) are stabilized by rotation, while the small structures ($|k| > k_R = 2\Omega^2 / \pi G \Sigma_0$) remain

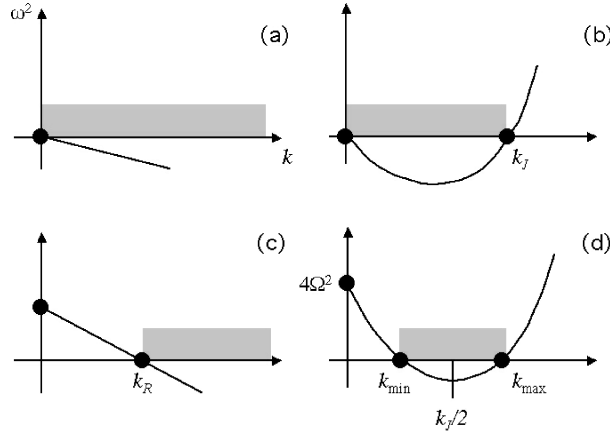


Fig. 2. Various cases of relation dispersions of free modes in rotating disks (3). In all panels, the grey intervals denote unstable mode regions. (a): motionless cold disk, (b): motionless hot disk, (c): rotating cold disk and (d): rotating hot disk. See text for details

unstable, see Fig. 2(c). This can be understood as large structures have a differential velocity in the disk due to the angular velocity Ω of the latter. As a consequence, a large structure which attempts to collapse under its own gravity will be stopped by the rotational barrier, when the centrifugal acceleration at its periphery balances its self gravity.

Note in passing that rotation does *not* stabilize the disk against all disturbances, as the smallest of them are still subject to gravitational collapses.

- *Hot rotating disk:* $c_s \neq 0$ and $\Omega \neq 0$. The dispersion relation $\omega^2 = k^2 c_s^2 - 2\pi G \Sigma_0 |k| + 4\Omega^2$ shows that ω^2 is minimum for $|k| = k_J/2 = \pi G \Omega_0 / c_s^2$, and that the minimum value is $\omega_{\min}^2 = 4\Omega^2 - \pi^2 G^2 \Sigma_0^2 / c_s^2$, as illustrated in Fig. 2(d).

It is convenient to define a dimensionless parameter, called the *Toomre parameter* ([9]):

$$Q = \frac{c_s \Omega}{\pi G \Sigma_0},$$

so that $\omega_{\min}^2 = (4\Omega^2 / Q^2) \cdot [Q^2 - 1/4]$. Thus, if $Q < 1/2$, then $\omega_{\min}^2 < 0$ and the disk remains unstable for an interval of wavenumbers (k_{\min}, k_{\max}) centered on $k_J/2$, see Fig. 2(d). Large structures (with small $|k|$) are then stabilized by rotation, while small structure (with large $|k|$) are stabilized by pressure. For

$$Q = \frac{c_s \Omega}{\pi G \Sigma_0} > \frac{1}{2},$$

the disk is stable to *any* disturbances. The above condition is called the Toomre criterium. Note that it is derived for a uniformly rotating disk. A

differentially rotating disk will also yield a similar criterium, except for the numerical coefficient in the right-hand side of the inequality.

Now, if a disk is rotating around a planet with potential Φ_P , then the equations of motion read (in a fixed frame this time):

$$\left\{ \begin{array}{l} \left(\frac{\partial}{\partial t} + \mathbf{v} \cdot \nabla \right) \mathbf{v} = -\nabla (\Phi_P + \Phi_D) - \frac{\nabla \cdot p}{\Sigma} \\ \frac{\partial \Sigma}{\partial t} + \nabla(\Sigma \mathbf{v}) = 0 \\ \nabla^2 \Phi_D = 4\pi G \Sigma \delta(z) \\ p = \Sigma c_s^2 \end{array} \right. \quad (4)$$

It is then more convenient to work with the radial and tangential components of the velocity, v_r and v_θ , respectively, instead of v_x and v_y . The price to pay is that v_r and v_θ now depend on θ , and this must be accounted for when applying the nabla operator ∇ . The linearization of the (4) then proceeds as before, and the new dispersion relation is:

$$\omega^2 = k^2 c_s^2 - 2\pi G \Sigma_0 |k| + \kappa^2, \quad (5)$$

where $\kappa = r^{-3} \partial [r^3 \partial \Phi_P / \partial r] / \partial r$ is the so-called epicyclic frequency, basically the frequency at which a particle oscillates horizontally around its average position (note that κ coincides with the mean motion n in the special case of a Keplerian potential $\Phi_P \propto -1/r$).

Equation (5) shows that the disk is stable against any disturbances if:

$$Q = \frac{c_s \kappa}{\pi G \Sigma_0} > 1, \quad (6)$$

which constitutes a more general version of the Toomre criterium. It illustrates quantitatively how pressure (c_s) and rotation (κ) tend to stabilize the disk against self-gravity (Σ_0).

5 Particle Size and Ring Thickness

In planetary rings, inelastic collisions tend to reduce the velocity dispersion c_s . This in turn decreases the value of Q below unity, leading to gravitational instabilities at some point, according to (6), and see Fig. 3. This causes the ring to collapse into small lumps. At that point, the finite mass and size of the lumps will maintain a small but non-zero velocity dispersion, of the order of the escape velocity at the surface of the largest particles,

$$c_s \sim \sqrt{G m_{\max} / R_{\max}},$$

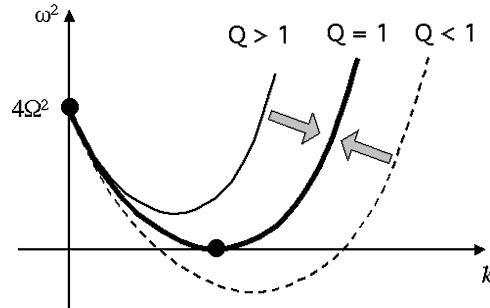


Fig. 3. Various cases of rotating hot disks: unstable ($Q < 1$), marginally stable ($Q = 1$) and stable for all modes ($Q > 1$). The arrows indicate that collisions and accretion tend to put the disk in the marginally stable state, see text

where m_{\max} and R_{\max} are the mass and radius of the largest lumps that dominate the dynamics of the ring. This allows the latter to maintain a Q value just above unity.

Conversely, if the lumps become too large, then the velocity dispersion increases and $Q > 1$, leading to an increase of dissipation and also to the disruption of the lumps. This will eventually decrease again the value of Q back to unity.

Thus, an equilibrium is reached, where a marginal stability is maintained ($Q \sim 1$), as illustrated in Fig. 3. This, combined with (6) and (5), leads to:

$$R_{\max} > \sim \left(\frac{a}{R_P} \right)^{3/2} \left(\frac{\Sigma_0}{100 \text{ g cm}^{-2}} \right) \left(\frac{\rho}{\text{g cm}^{-3}} \right)^{1/2} \text{ meters ,}$$

where a is the distance to the planet center and ρ is the bulk density of the largest particles.

As an example, if we take typical values of $\Sigma_0 \sim 20 \text{ g cm}^{-2}$ corresponding to Saturn's A ring, $\rho < \sim 1 \text{ g cm}^{-3}$ for icy particles and $a \sim 2R_P$, this yields $R_{\max} > \sim$ of a few meters, in accordance with radio *Voyager* observations.

More generally, the thickness h of the ring is given by $h \sim c_s/\Omega$, where the orbital angular velocity $\Omega \sim \kappa \sim \sqrt{GM_P/a^3}$ in a Keplerian disk. Also, a homogeneous ring of radius a has a mass of $m_r \sim \pi \Sigma_0 a^2$. Combining these relations with the expression of Q yields:

$$\frac{h}{a} \sim Q \times \frac{m_r}{M_P} . \quad (7)$$

Thus, we see that the thickness of a marginally stable ring is eventually imposed by the ratio of the ring mass to the planet mass: the extreme thinness of planetary rings comes from their extremely small mass when compared to the planet. For Saturn's A ring, with $m_r/M_P \sim 10^{-7}$, we obtain $h \sim$ a few meters, in agreement again with (indirect) measurements of h , see Sect. 7.

Note for closing this section that the first marginally unstable modes, appearing when $Q \sim 1$, corresponds to the minimal value of ω^2 in (5). They have wavenumbers $k_{\text{unst}} \sim k_J/2 \sim \Omega/c_s$, i.e. wavelengths:

$$\lambda_{\text{unst}} \sim 2\pi h ,$$

or a few tens of meters. These marginal instabilities are probably the explanation for the quadrant asymmetries observed in Saturn's A ring.

6 Resonances in Planetary Rings

So far, we have been considering *free* modes propagating in rings. We now turn to the case where modes are *forced* by a satellite near a resonance.

Considering the very small masses of the satellites relative to the giant planets, these forced modes are in general “microscopic”, in the sense that they induce deviations of a few meters on the particles orbits. However, near resonances, a satellite can excite macroscopic responses in the disk, which exhibit large collective disturbances over tens of kilometers, i.e. on scales observable by spacecraft imagers.

As explained later, this collective response allows an secular exchange of angular momentum and energy between the ring and the satellite, very much like tides allow secular exchanges between a planet and its satellites.

The equations of motion are the same as in (4), except that the first equation (Euler's) must now accounts for the forcing of the satellite through its disturbing potential Φ_S :

$$\left\{ \begin{array}{l} \left(\frac{\partial}{\partial t} + \mathbf{v} \cdot \nabla \right) \mathbf{v} = -\nabla (\Phi_P + \Phi_D + \Phi_S) - \frac{\nabla \cdot \mathbf{P}}{\Sigma} \\ \frac{\partial \Sigma}{\partial t} + \nabla(\Sigma \mathbf{v}) = 0 \\ \nabla^2 \Phi_D = 4\pi \Sigma G \delta(z) \\ p = \Sigma c_s^2 , \end{array} \right. \quad (8)$$

Note in passing that we have replaced the (scalar) isotropic pressure p by a pressure tensor, \mathbf{P} . This allows us to take into account in a general way more complicated effects like viscosity or non-isotropic pressure terms.

The simplest case we can think of is the forcing of a homogeneous disk by a small satellite of mass $m_s \ll M_P$ with a circular orbit of radius a_s and mean motion n_S around a point-like planet with potential $\Phi_P(r) = -GM_P/r$. This is the Keplerian approximation. In reality, the oblateness of the planet introduces extra terms causing a slow precession of the apse and node of the orbit. These subtleties will not be taken into account here since they obscure our

main point (the study of a simple isolated resonance) without changing our main conclusions. These effects would become important, however, if the orbital eccentricity and inclination of the satellite were to come into play.

With these assumptions, the satellite potential is periodic in $\theta - n_S t$, so that it can be Fourier expanded as:

$$\Phi_S(r, \theta, t) = \sum_{m=-\infty}^{+\infty} \Phi_{Sm}(r) \cdot \exp[im(\theta - n_S t)] , \quad (9)$$

where m is an integer, $\Phi_{Sm}(r) = -(Gm_S/2a_S) \cdot b_{1/2}^m(r/a_S)$ and $b_{1/2}^m$ is the classical Laplace coefficient (see [12] for a review of the properties of these coefficients). We note that $\Phi_m(r) = \Phi_{-m}(r)$, since Φ_s is real.

Equations (8) are then linearized, and we assume that the free modes of the disk are damped by collisions, or are at least negligible with respect to the forced modes, especially near the resonances. Then all the perturbed quantities, for instance the radial velocity v_r , take the same form as the forcing (9), i.e. $v_r(r, \theta, t) = \sum v_{rm}(r) \cdot \exp[jm(\theta - n_S t)]$, etc..

Each term $\Phi_{Sm}(r) \cdot \exp[jm(\theta - n_S t)]$ of the satellite potential then forces a mode in the ring, and if equations (8) remain linear, then it is enough to study the reaction of the disk to each mode separately. As already noted before, this replaces the differential operators by mere multiplications, namely $\partial/\partial t = -jmn_s$ and $\partial/\partial \theta = jm$.

This approach is especially useful near resonances, where one mode dominates over all the other ones, and can thus be “clipped off” from the rest. Consider a particle with mean motion n , so that its longitude writes $\theta = nt$ (plus an arbitrary constant). This particle thus feels a forcing potential $\Phi_{Sm}(r) \cdot \exp[jm(\theta - n_S t)] = \Phi_{Sm} \exp[jm(n - n_S)t]$, i.e. a term with frequency $m(n - n_S)$.

A so-called (“Excentric Lindblad Resonance”) (ELR) occurs when this frequency matches the horizontal epicyclic frequency κ of the particle, i.e. when:

$$\kappa = \pm m(n - n_S) . \quad (10)$$

In this case, and for small horizontal displacements of the particle, the latter behaves very much like a harmonic oscillator (i.e. a linear system) near a classical resonance. This simple model predicts that the horizontal displacement of the particle increases as it approaches the resonance, and becomes singular at exact resonance¹. In reality, non-linear terms come into play in the disk and eventually prevent the singularity. In counterpart, this complicates significantly the equations of motion, and renders the system rather untractable.

Fortunately, for sufficiently dense planetary rings perturbed by very small satellites, collisions, pressure and self-gravity prevent a wild behavior for

¹This horizontal displacement is proportional to the orbital eccentricity of the particle, hence the nomenclature “Excentric Lindblad Resonance”

nearby streamlines, thus keeping the perturbed motion small, and eventually ensuring that the system 8 remains linear.

Note that for a Keplerian disk $\kappa = n$, so that the condition $\kappa = \pm m(n - n_s)$ is equivalent to

$$n = \frac{m}{m \mp 1} \cdot n_s, \quad (11)$$

corresponding to mean motion resonances 2:1, 3:2, 4:3, etc..., also called first order resonances. Other resonances, e.g. second order resonances 3:1, 4:2, 5:3 (i.e. of the form $m : m - 2$) can also come into play when the smaller second order terms in the particle orbital eccentricity are considered. Still other resonances (referred to as ‘‘corotation resonances’’) can also arise when the satellite orbital eccentricity is accounted for. These kinds of resonances fall outside the main topic of this chapter and will not be considered here.

Another important simplification comes from the fact that in planetary rings, the perturbed quantities vary much more rapidly radially than azimuthally. Physically, this means that the spiral structures resonantly forced are *tightly wound*, like the grooves of a music disk. More precisely, the lower order radial derivatives can be neglected with respect to higher orders:

$$\frac{m^2}{r^2} \ll \frac{m}{r} \cdot \frac{d}{dr} \ll \frac{d^2}{dr^2}. \quad (12)$$

This is the WKB approximation², which greatly simplifies the system 8, leading to (see [13]):

$$\left\{ \begin{array}{l} jm(n - n_s)v_{rm} - 2nv_{\theta m} = -\dot{\Phi}_{Sm} - \dot{\Phi}_{Dm} - \frac{c_s^2 \dot{\sigma}_m}{\Sigma_0} + \left(\mu + \frac{4\nu}{3}\right)\ddot{v}_{rm} \\ \frac{n}{2}v_{rm} + jm(n - n_s)v_{\theta m} = -jm\frac{\Phi_{Sm} + \Phi_{Dm}}{r} - jm\frac{c_s^2 \sigma_m}{r\Sigma_0} + \nu\ddot{v}_{\theta m} \\ \sigma_m = -\frac{\Sigma_0 \dot{v}_{rm}}{jm(n - n_s)} \\ \dot{\Phi}_{Dm} = -2\pi Gjs\sigma_m \\ p_m = c_s^2 \sigma_m. \end{array} \right. \quad (13)$$

The quantities μ and ν are the bulk and shear kinematic viscosities, respectively, coming from the pressure tensor \mathbf{P} . The dot stands for the *space* (not time) derivative d/dr . The Poisson equation has been solved using the results of [12], where $s = \pm 1$ is chosen in such a way that the disk potential out of the disk plane tends to zero:

$$\Phi_{Dm}(r + is|z|) \rightarrow 0, \quad (14)$$

²Developed by Wentzel-Kramer-Brillouin in the field of quantum mechanics.

as $|z|$ goes to infinity. We will see that boundary conditions actually impose $s = +1$.

If we forget for the moment the terms Φ_{Dm} , σ_m , μ and ν , i.e. if we consider a test disk with no self-gravity, no pressure nor viscosity, then we get:

$$\begin{cases} v_{rm}(r) = -jm \left[(n - n_s)r \frac{d}{dr} + 2n \right] \cdot \Phi_{Sm}(r) \frac{1}{rD} \\ v_{\theta m}(r) = \left[nr \frac{d}{dr} + 2m^2(n - n_s) \right] \cdot \Phi_{Sm}(r) \frac{1}{2rD} \end{cases} \quad (15)$$

where $D(r) = n^2 - m^2(n - n_s)^2$ is a measure of the distance to exact resonance. The velocity is singular when $D = 0$, i.e. when $n = m/(m \mp 1)n_s$, corresponding to the condition (11). Thus the dependence in $1/D$ is just the expected response of a linear oscillator near a resonance.

The result obtained above does not strike by its simplicity: complicated equations and tedious calculations have just shown that a harmonic oscillator behaves as derived in basic text books. However, we have gained with these equations some important insights into more subtle effects associated with viscosity, pressure and self-gravity. More generally, these equations show how *collective* effects modify the simple harmonic oscillator paradigm into more complicated behaviors.

Near the resonance, $D = 0$, the system 13 is almost degenerate, and (15) yield $u_{\theta m} \sim \pm(j/2)u_{rm}$. To solve for u_{rm} , one uses this degeneracy, plus the tightly wound wave condition (12). We note x the relative distance to the resonance radius a_m , $x = (a - a_m)/a_m$, and we expand (13) near $x = 0$, which yields:

$$-\alpha_v^3 \frac{d^2}{dx^2}(u_{rm}) + \alpha_G^2 \frac{d}{dx}(u_{rm}) - jxu_{rm} = C_m, \quad (16)$$

where:

$$\begin{cases} \alpha_v^3 = j\alpha_P^3 + \alpha_\nu^3 \\ \alpha_P^3 = \mp \frac{c_s^2/n}{3ma_m^2 n_s} \\ \alpha_\nu^3 = \frac{\mu + 7\nu/3}{3ma_m^2 n_s} \\ \alpha_G^2 = \pm \frac{2\pi s G \Sigma_0}{3ma_m n n_s} \end{cases}, \quad (17)$$

and C_m is a factor which weakly depends on m ([13]). For purposes of numerical applications, $C_m \sim \pm 0.27an(m_s/M)$ as m tends to infinity. The coefficient $C_m \propto m_s$ in (16) is the forcing term due to the satellite. The coefficients α_P , α_ν and α_G encapsulate the effects of pressure, viscosity and self-gravitation, respectively. In the absence of all the α 's, the response of the disk is indeed

singular at the resonance $x=0$: $u_{rm} \propto 1/x$, as expected in a test disk in the linear regime. The extra terms with the α 's in (16) prevent such an outcome, and forces the solution to remain finite at $x = 0$. If oscillations are present in the solution, then waves are launched.

Equation (16) can be solved by defining the Fourier transform of u_{rm} :

$$\tilde{u}_{rm}(k) = \int_{-\infty}^{+\infty} \exp(-jkx)u_{rm}(x)dx ,$$

assuming that $u_{rm}(x)$ is square integrable. Then we take the Fourier transform of (16):

$$\frac{d}{dk}(\tilde{u}_{rm}) + (\alpha_v^3 k^2 + j\alpha_G^2 k)\tilde{u}_{rm} = 2\pi C_m \delta(k) , \quad (18)$$

where δ is the Dirac function. This first-order equation is solved with the boundary condition $\tilde{u}_{rm} \rightarrow 0$ as $k \rightarrow \infty$, since \tilde{u}_{rm} is a Fourier transform. Then:

$$\tilde{u}_{rm}(k) = 2\pi C_m H(k) \exp[-(\alpha_v^3 k^3/3 + j\alpha_G^2 k^2/2)] ,$$

where H is the unit-step function ($=0$ for $k < 0$ and $=1$ for $k > 0$). This eventually provides the solution we are looking for:

$$u_{rm}(x) = C_m \int_0^{+\infty} \exp[j(kx - \alpha_G^2 k^2/2 - \alpha_P^3 k^3/3) - \alpha_v^3 k^3/3] dk . \quad (19)$$

Note that the boundary condition (14) also requires $u_{rm}(x + is|z|) \rightarrow 0$ as $|z| \rightarrow +\infty$, i.e. $s = +1$ since $k > 0$ in the integral above.

The qualitative behavior of $u_{rm}(x)$ can be estimated from the behavior of the argument in the exponential, $j(kx - \alpha_G^2 k^2/2 - \alpha_P^3 k^3/3) - \alpha_v^3 k^3/3$. This argument has an imaginary part, $j(kx - \alpha_G^2 k^2/2 - \alpha_P^3 k^3/3)$, which causes an oscillation of the function in the integral, and a real part, $-\alpha_v^3 k^3/3$, which causes a damping of that function.

The integral in (19) is significant only when the phase $kx - \alpha_G^2 k^2/2 - \alpha_P^3 k^3/3$ is stationary, i.e. near the wave number k_{stat} such that:

$$\alpha_G^2 k_{\text{stat}} + \alpha_P^3 k_{\text{stat}}^2 = x \quad (20)$$

somewhere in the domain of integration ($k > 0$).

For instance, if the disk is dominated by self-gravity, i.e. $\alpha_G^2 \gg \alpha_P^3$, then the condition (20) reduces to $x = \alpha_G^2 k_{\text{stat}}$. Thus, the integral in (19) is significant only on that side of the resonance where x and α_G^2 have the same sign. In that case, the solution of 19 oscillates near x with a local radial wave number $k_{\text{stat}} \approx x/\alpha_G^2$. The local radial wavelength of the wave is thus $\propto 1/x$. Consequently, the wave oscillates more and more and more rapidly as it propagates away from the resonance, see Fig. 4(a). On the other side of the resonance (where x and α_G^2 have opposite signs), the argument of the exponential in (19) is never stationary, and the integral damps to zero. This means that the

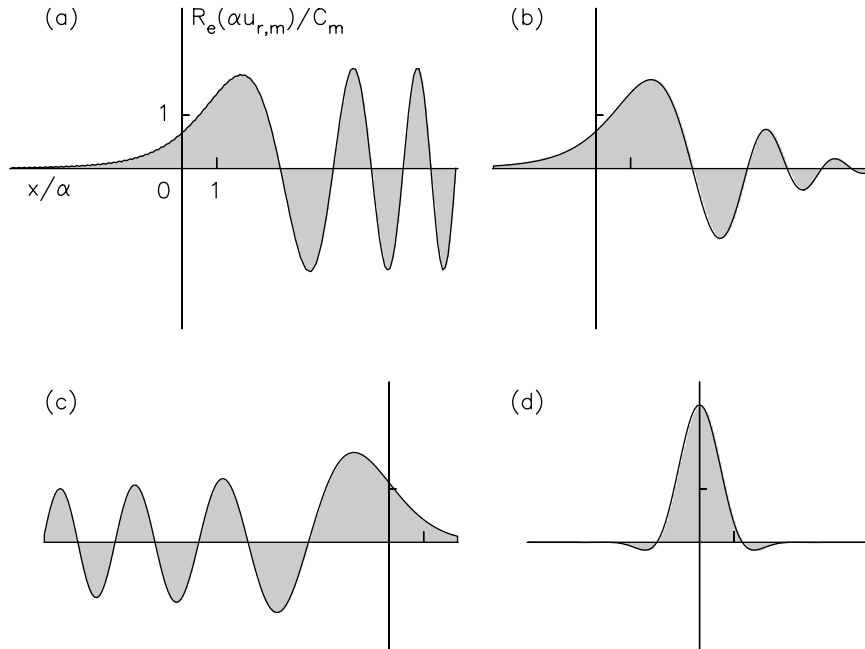


Fig. 4. Various responses of a disk near an inner Lindblad resonance (located at $x = 0$). The term α which appears in the definition of the abscissa and ordinate units represents any of the coefficients defined in (17), depending on the case considered. (a) A disk dominated by self-gravity. The wave is launched at $x = 0$ and propagates to the right of the resonance, while remaining evanescent on the left side. (b) A self-gravity wave damped by viscosity. (c) A wave in a disk dominated by pressure. The propagating and evanescent sides are inverted with respect to the self-gravity case. (d) Response in a disk dominated by viscosity. The wave is now evanescent on both sides of the resonance

wave is evanescent, with a typical damping distance of $\sim |\alpha_G|$ in the forbidden region, see again Fig. 4(a).

The same reasoning shows that when the disk is dominated by pressure ($\alpha_P^3 \gg \alpha_G^2$), then the wave propagates on the side of the resonance where x and α_P^3 have the same sign. The local radial wave number is now $k_{\text{stat}} \approx \sqrt{x/\alpha_P^3}$, and the local radial wavelength is $\propto 1/\sqrt{x}$. Again the wave oscillates more and more rapidly as it goes away from the resonance, but not so drastically as for a wave supported by self-gravity, see Fig. 4(c). When x and α_P^3 have opposite signs, the wave is evanescent over a damping distance of $\sim |\alpha_P|$.

The effect of viscosity is illustrated in Figs. 4(b) and 4(d). In case (b), viscosity remains weak enough to allow for a few self-gravity waves to propagate in the disk. In case (d), viscosity completely dominates the disk response, and no wave can be launched from the resonance.

7 Waves as Probes of the Rings

It is interesting to compare the numerical values of the coefficients α_G and α_P for planetary rings. The larger of the two coefficients tells us which process (self-gravity or pressure) dominates in the wave propagation. According to the expressions given in (17), using the definition of Toomre's parameter, $Q = c_s n / \pi G \Sigma_0$, and remembering that the thickness of the ring is given by $h \sim c_s / n$, we obtain:

$$\left| \frac{\alpha_P}{\alpha_G} \right| \sim \sqrt{2Q} \left(3m \frac{h}{a} \right)^{1/6}.$$

As we saw before, $h/a \sim 10^{-7}$ is very small and $Q \sim 1$, while m is typically a few times unity. Thus, the ratio $\alpha_P/\alpha_G \sim 0.1 - 0.2$ is small, but not by an overwhelming margin, because of the exponent 1/6 in the expression above.

The same is true with the ratio α_ν/α_G since $\alpha_\nu \sim \alpha_P$. This is because the kinematic viscosities μ and ν are both of the order of c_s^2/n is moderately thick planetary rings ([2]).

Consequently, self-gravity is the dominant process governing the propagation of density waves in planetary rings, but viscosity is efficient enough to damp the wave after a few wavelengths, see for instance the panel (b) in Fig. 4.

Note that self-gravity waves are macroscopic features which can be used as a probe to determine microscopic parameters such as the local surface density Σ_0 of the ring, or its kinematic viscosities μ or ν . This method has been used with bending waves in Saturn's A ring and is the only way so far to derive Σ_0 or ν in these regions ([5]).

The determination of ν has an important consequence, namely the estimation of the local thickness h of the ring, since $\nu \sim c_s^2/n$. Typical values obtained for Saturn's A ring indicate that $h \sim 10 - 50$ meters, a value already consistent with stability considerations, see for instance the discussion after Eq. (7).

8 Torque at Resonances

A remarkable property of the function $u_{rm}(x)$ defined in (19) is that the real part of its integral, $\Re[\int_{-\infty}^{+\infty} u_{rm}(x) dx]$, is *independent* of the values of the coefficients α 's. For instance, all the areas under the curves of Fig. 4 (i.e. the shaded regions) are equal, *including* in the cases (c) and (d), where dissipation plays an important role.

This can be shown by using an integral representation of the step function ([13]),

$$H(k) = (j/2\pi) \int_{-\infty}^{+\infty} [exp(-jku)/(u + j\epsilon)]$$

in (19), where ϵ is an arbitrarily small number. Equation (19) may then be then integrated in x , which yields $\delta(k)$, then in k , and finally in u :

$$\Re \left(\int_{-\infty}^{+\infty} u_{rm} dx \right) = \Re \left(j C_m \int_{-\infty}^{+\infty} \frac{du}{u + j\epsilon} \right) = \pi C_m . \quad (21)$$

Now, the complex number $u_{rm}(x)$ describes how the disk responds to the resonant excitation of the satellite at the distance x from the resonance. More precisely, the modulus $|u_{rm}(x)|$ is a measure of the amplitude of the perturbation at x , and is thus directly proportional to the eccentricity of the streamlines around x . The argument $\phi = \arg[u_{rm}(x)]$ is on the other hand directly connected to the phase lag Ψ of the perturbation with respect to the satellite potential. It can be shown easily that $\phi = \Psi \mp \pi/2$, see [13].

Consequently, the satellite torque acting on a given streamline is proportional to its eccentricity $\propto |u_{rm}(x)|$ and to $\sin(\Psi) \pm \cos(\phi)$, a classical properties of linear oscillators. Consequently the total torque exerted at the resonance is proportional to $\Re[\int_{-\infty}^{+\infty} u_{rm}(x) dx]$.

More precisely, the torque exerted by the satellite on the disk is by definition $\Gamma = \int \int (\mathbf{r} \times \nabla \Phi_S) \Sigma d^2 r$, where Φ_S and Σ may be Fourier expanded according to (9) when the stationary regime is reached. After linearization, one gets the torque exerted at the resonance:

$$\Gamma_m = \mp 12\pi m^2 \Sigma_0 a_s^2 C_m \Re \left(\int_{-\infty}^{+\infty} u_{rm}(x) dx \right), \quad (22)$$

where the upper (resp. lower) sign applies to a resonance inside (resp. outside) the satellite orbit.

This is the so-called ‘‘standard torque’’ ([1]), originally derived for a self-gravity wave launched at an isolated resonance. The calculations made above show that this torque is actually *independent* of the physical process at work in the disk, as long as the response of the latter remains linear. In particular, dissipative processes such as viscous friction do not modify the torque value.

This torque allows a secular exchange of angular momentum between the disk and the satellite. Note that the sign of this exchange is such that the torque always tends to push the satellite away from the disk.

This torque have a wide range of applications that we will not review here. We will just note here that it may lead to the confinement of a ring when two satellites lie on each side of the latter (the so-called ‘‘shepherding mechanism’’). This could explain for instance the confinement of some of the narrow Uranus’ rings.

Another consequence of such a torque is that Saturn’s rings and the inner satellites are continuously pushed away from each other. The time scales associated with such interactions (of the order of 10^8 years) tend to be shorter than the age of the solar system ([2]). This suggests that planetary rings are either rather young, or, if primordial, have continuously evolved and lived several cycles since their formation.

9 Concluding Remarks

We have considered in this chapter some fundamental concepts associated with rings: their flattening, their thickness and their resonant interactions with satellites. Note that these processes are mainly linked to the larger particles of the rings. Furthermore, they make a useful bridge between the microscopic and macroscopic properties of circumplanetary disks.

Meanwhile, many other processes have not been discussed here, such as the effect of electromagnetic forces on dust particles, the detailed nature of collisions between the larger particles, the accretion and tidal disruption of loose aggregates of particles, the origin of sharp edges in some rings, their normal modes of oscillation, etc. . .

These issues, and others, are addressed in some of the references given in the bibliography below. All the processes involved clearly show that rings are by no means the simple and everlasting objects they seem to be when observed from far away.

References

1. P. Goldreich, S. Tremaine: *Ann. Rev. Astron. Astrophys.* **20**, 249 (1982)
2. N. Borderies, P. Goldreich, S. Tremaine: unsolved problems in planetary ring dynamics. In: *Planetary rings*, ed by R. Greenberg, A. Brahic (Univ. Of Arizona Press 1984) pp 713–734
3. P.D. Nicholson, L. Dones: *Rev. Geophys.* **29**, 313 (1991)
4. P. Goldreich: puzzles and prospects in planetary ring dynamics. In: *Chaos, resonance and collective dynamical phenomena in the solar system*, ed by S. Ferraz-Mello (Kluwer Academic Publishers, Dordrecht Boston London 1992) pp 65–73
5. L.W. Esposito: *Annu. Rev. Earth Planet. Sci.* **21**, 487 (1993)
6. J.N. Cuzzi: *Earth, Moon, and Planets* **67**, 179 (1995)
7. A.W. Harris: the origin and evolution of planetary rings. In: *Planetary rings*, ed by R. Greenberg, A. Brahic (Univ. Of Arizona Press 1984) pp 641–659
8. W. Ward: the solar nebula and the planetesimal disk. In: *Planetary rings*, ed by R. Greenberg, A. Brahic (Univ. Of Arizona Press 1984) pp 660–684
9. A. Toomre: *ApJ.* **139**, 1217 (1964)
10. J. Binney, S. Tremaine: *Galactic Dynamics* (Princeton University Press 1988)
11. P.Y. Longaretti: Planetary ring dynamics: from Boltzmann’s equation to celestial dynamics. In: *Interrelations between physics and dynamics for minor bodies in the solar system*, ed by D. Benest, C. Froeschlé (Editions Frontières, Gif-sur-Yvette 1992) pp 453–586
12. F.H. Shu: waves in planetary rings. In: *Planetary rings*, ed by R. Greenberg, A. Brahic (Univ. of Arizona Press 1984) pp 513–561
13. N. Meyer-Vernet, B. Sicardy: *Icarus* **69**, 157 (1987)
14. B. Sicardy: Planetary ring dynamics: Secular exchange of angular momentum and energy with a satellite. In: *Interrelations between physics and dynamics for minor bodies in the solar system*, ed by D. Benest, C. Froeschlé (Editions Frontières, Gif-sur-Yvette 1992) pp 631–651